European Journal of Medicinal Chemistry 44 (2009) 1230–1239

Contents lists available at ScienceDirect

European Journal of Medicinal Chemistry

journal homepage: http://www.elsevier.com/locate/ejmech

Original article

Natural polyprenylated benzophenones inhibiting cysteine and serine proteases

Felipe T. Martins [a,*], Diego M. Assis [a], Marcelo H. dos Santos [a], I. Camps [a], Márcia P. Veloso [a], Maria A. Juliano [b], Lira C. Alves [a], Antônio C. Doriguetto [a]

[a] Department of Exact Science, Federal University of Alfenas, Rua Gabriel Monteiro da Silva 714, Alfenas, MG 37130-000, Brazil
[b] Department of Biophysics, Federal University of São Paulo, Rua Três de Maio 100, CP 369, São Paulo, SP 04044-020, Brazil

ARTICLE INFO

Article history:
Received 3 May 2008
Received in revised form 7 August 2008
Accepted 4 September 2008
Available online 24 September 2008

Keywords:
Benzophenones
Proteases
Guttiferone A
Cathepsin G
SAR
Flexible docking

ABSTRACT

We have investigated the in vitro inhibition of papain, trypsin, and cathepsins B and G by five benzophenone-type compounds, three natural ones isolated from *Garcinia brasiliensis* and two synthetic derivatives. The activities of pentaprenylated trihydroxy-substituted benzophenone guttiferone A (**1**) on all assayed enzymes were approximately 2–69 folds higher than that manifested by mono-hydroxylated tetraprenylated and triprenylated compounds epiclusianone (**2**) and garciniaphenone (**3**), respectively, the other natural benzophenones that also inhibited significantly the four enzymes. Differently, the synthetic derivatives 2,2′,4-trihydroxybenzophenone (**4**) and diphenylmethanone (**5**) have inhibited weakly the studied proteases. Furthermore, compound **1** has bonded preferentially to cathepsin G, once its IC_{50} value (2.7 ± 0.1 μM) on such peptidase is quite similar to that of the classical inhibitor of serine proteases, chymostatin (2.1 ± 0.1 μM). Interesting structure–activity relationships (SARs) were confirmed by flexible docking simulations, likewise the potential usefulness of natural compound **1** as antitumoral drug is strengthened by our results concerning the antiproteolytic activity.

1. Introduction

Proteases or peptidases are enzymes that catalyze reactions on peptide chains, hydrolyzing them into short fragments by splitting the peptide bond between amino acid residues placed either within the ribbon, in this case they are known as endopeptidases, or at the polymeric backbone end (exopeptidases). These enzymes can be further joined according to the reactant groups that are present in the catalytic site, as the serine (EC 3.4.21), cysteine (EC 3.4.22), aspartic acid (EC 3.4.23), metalo (EC 3.4.24) and threonine (EC 3.4.25) proteases. Papain (EC 3.4.22.2), a plant cysteine protease isolated from *Carica papaya* latex, cleaves preferentially peptide chains on either Arg and Lys residues or hydrophobic Phe ones [1]. The cathepsins, a group of lysosomal enzymes, are proteases presenting several members. Two of them, cathepsin B (CatB, EC 3.4.22.1) and cathepsin G (CatG, EC 3.4.21.20), have been identified in human tissues, where they can be isolated [2]. CatB, a papain-like protease, is barely detected in the extracellular matrix, at least in nonpathological tissues, due to its low stability in neutral–alkaline pH values [3,4]. Concerning the neoplastic events, CatB is secreted out of the cells and it presents essentially an endopeptidase-functioned proteolytic activity crucial to tissue rupture around the tumor spreading area and metastasis [5–7]. Moreover, high expression, activity and secretion of CatB have been observed in several types of tumors, such as breast, gastric, lung and prostate ones [8]. The CatG is the major serine protease in the azurophilic granules of polymorphonuclear leukocytes [9,10] and is involved in the degradation of foreign bodies and injured tissues enclosed by phagosomal vesicles during inflammatory responses [11]. In opposition to CatB, CatG is commonly released towards the extracellular matrix. Its proteolytic activity is finely controlled by serum proteinase inhibitors, which can fail quantitatively or qualitatively in down-regulation due to genetic or acquired deficiencies resulting in a disturbed digestion of extracellular proteins that could contribute to the development of connective tissue diseases, such as emphysema, rheumatoid arthritis and perionditis [12]. Furthermore, recent evidences have suggested that this lysosomal protease presents alternative physiologic roles, as for instance platelet activation [13], monocyte and neutrophil chemotaxis [14], natural killer cytotoxicity increasing [15], proteolytic processing of interleukin-8 [16], complement C3 [17] and factor V [18], as well as other pathological ones, such as dissemination of tumor aggregates from

Abbreviations: CC, column chromatography; TLC, thin layer chromatography; MAP, mitogen-activated protein; XRD, X-ray diffraction; HPLC, High Performance Liquid Chromatography; Z-FR-AMC, carbobenzyloxy-Phe-Arg-(7-amino-4-methylcoumarin); EDTA, ethylenediaminetetraacetic acid; DMSO, dimethyl sulfoxide; DTT, dithiothreitol; LP, leupeptin; E-64, 1-[[(L-*trans*-epoxysuccinyl)-L-leucyl]amino]-4-guanidinobutane; SBTI, soybean trypsin inhibitor; Abz-, *ortho*-aminobenzoic acid; -EDDnp, *N*-(ethylenediamine)-2,4-dinitrophenyl amide; IC_{50}, inhibitor concentration to decrease 50% enzymatic activity; VDW, van der Waals.

* Corresponding author. Tel. +55 35 33991261. fax: +55 35 32991262
E-mail address: felipetmartins@yahoo.com.br (F.T. Martins).

0223-5234/$ – see front matter © 2008 Elsevier Masson SAS. All rights reserved.
doi:10.1016/j.ejmech.2008.09.018

primary tumor sites after to be secreted out by infiltrated neutrophils [19].

Trypsin (E.C. 3.4.21.4) has specificity for peptides containing Arg and Lys residues and its catalytic triad is composed of the amino acids serine, histidine and aspartate, in the same way that occurs in similar serine proteases [20]. Each amino acid of the triad has a specific role in the peptide bond cleavage of the substrates, wherein the carboxylate group of the aspartic acid is hydrogen bonded to the amine nitrogen atom of the histidine residue, contributing to increase the electronegativity of the imine nitrogen within the same heterocyclic side chain. In this way, the free electron pair of this last imidazolyl nitrogen atom is devoted to accept the hydrogen from the serine hydroxyl group, powering, therefore, the nucleophilic attack by this serine residue on the carbonyl carbon atom of the peptide bond that is properly oriented into the enzymatic active site. Cysteine proteases have a similar catalytic mechanism with a nucleophilic cysteine thiol group. In Fig. 1, a simplified nucleophilic attack scheme of serine and cysteine proteases is illustrated. After the peptide carbonyl group to be nucleophilically attacked, in a following step, the amide bond is cleaved due to an electronic rearrangement and the acyl-protease intermediate is generated. To release the free enzyme, a water molecule, in place of the N-terminal end of the cleaved peptide, attacks the carbonyl carbon keeping bonded the substrate–enzyme complex, resulting in the formation of a binding between the water oxygen atom and the peptide carbon one. Here, it should be highlighted that the imine nitrogen of the histidine residue plays an important role by accepting a proton from water. At last, the bond formed in the initial step between the serine and the carbonyl carbon is broken and the C-terminus of the substrate leaves then. We recommend consulting the literature for an overall approach on such hydrolase groups [20].

Our research group has dealt with synthetic and natural benzophenone derivatives regarding structural elucidation and screening for pharmacological properties on various biological systems. From the *Garcinia brasiliensis* fruits and seeds, three benzophenones possessing a polyprenylated bicyclo[3.3.1]-nonane-2,4,9-trione core were isolated through repeated column chromatography (CC), repeated preparative thin layer chromatography (TLC) and recrystallizations in methanol solutions: guttiferone A (**1**), an anti-HIV compound that was initially isolated in 1992 [21]; epiclusianone (**2**), a vasoactive substance identified in 1998 [22] that also presents effects against HIV infection [23,24]; and garciniaphenone (**3**), a first example of natural benzophenone presenting just three prenyl moieties that has been discovered for the first time in this plant by us. A trihydroxylated benzophenone named systematically (2,4-dihydroxyphenyl)(2-hydroxyphenyl)methanone, or simply 2,2′,4-trihydroxybenzophenone (**4**), was previously synthesized in our laboratories by aromatic electrophilic substitution [25]. All these benzophenone derivatives were spectroscopically featured and their structures have been accurately determined via single crystal X-ray diffraction techniques [22,26,27], likewise the anti-inflammatory and antioxidant properties were recently described for such natural products [25]. Furthermore, the polyisoprenylated benzophenone derivatives of the bicycle[3.3.1]-nonanetrione moiety are implicated in the inhibition of DNA topoisomerases and telomerase and also act as regulators within mitogen-activated protein (MAP) kinase signal transduction pathways, decreasing mitosis rate in cancerous and tumoral tissues, once MAP kinases are active enzymes during mitosis process [28]. Due to their merged effects on different pharmacological targets for antineoplastic therapy, the natural benzophenones in query can be useful as antitumoral compounds (Scheme 1).

As above mentioned, proteases are potentially involved in many diseases, including tumor growth and spreading and HIV maturation due to interaction with HIV-1 gp120 protein V3 loop [29]. Therefore, these enzymes are molecularly searched for more effective drugs that could be employed in the therapeutic. However, a notable challenge involved in the design and development of protease inhibitors has consisted to add properties such as high enzymatic inhibition rates and suitable bioavailability in a single molecule [30]. Several potent peptide inhibitors are available, whereas these compounds fail to satisfy the pharmacokinetic requirements in view of high hydrophilicity and hydrolysable moieties present in their structures. Thereby, small non-peptide molecules are currently preferred to survey novel antiproteolytic drugs. In this work, we have reported the in vitro inhibition of model enzymes of cysteine and serine proteases, papain and trypsin, respectively, CatB and CatG by four benzophenone derivatives presenting lipophilic character appropriate to cross biological membranes, which would make possible the use of most active assayed benzophenones as pharmaceutical ingredients. In addition, the results obtained with flexible docking simulations have shown interesting structure–activity relationships and can be useful in the rationalizing of the anti-HIV effect presented by these compounds.

2. Chemistry

The natural polyprenylated benzophenones **1** and **3** were isolated from the ethanolic and hexanic extracts of *G. brasiliensis* dried and powdered seeds (700 g) and fruits (1000 g), respectively, whereas compound **2** was obtained from both prior extracts. Chromatographic efforts on thin layer plates and filled columns have been employed in order to achieve the isolation of these compounds. For purification, several recrystallizations in methanol solution were performed to give 0.51, 2.80 and 0.65 g of **1**–**3**, respectively, which were characterized by spectroscopic methods (UV, IR, MS, 1D and 2D spectra of ^{1}H and ^{13}C NMR) and their intra- and inter-molecular geometries in the solid state were entirely determined and

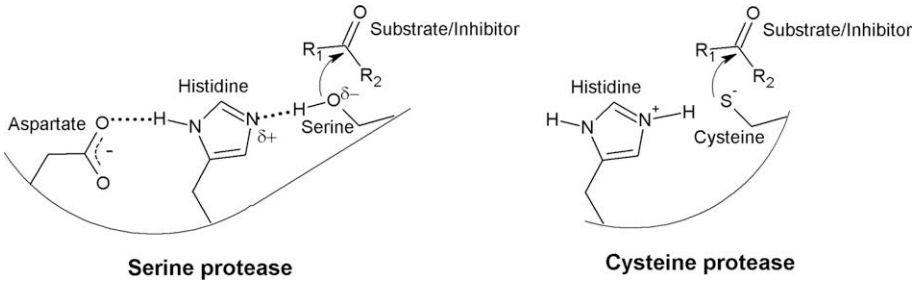

Fig. 1. A general view of the nucleophilic attack mode whereby serine and cysteine proteases either catalyze the hydrolysis of peptide backbones or bond irreversibly to some inhibitors. The side chains are shown for the amino acid residues which are well conserved into the enzymatic active site of these two protease classes. The arrows indicate the nucleophilic attack by the oxygen and sulfur atoms from serine and cysteine residues, respectively, on the electronically deficient carbonyl carbon of the peptide substrates and of various covalently bonded inhibitors.

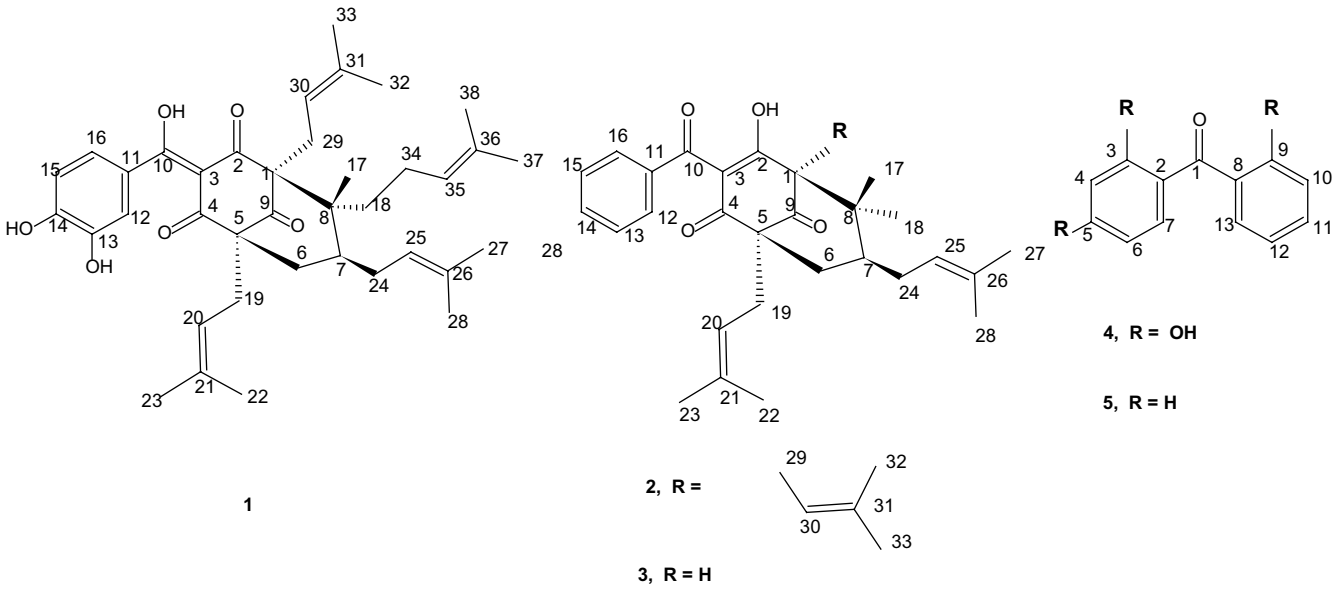

Scheme 1. Chemical structures of benzophenones guttiferone A (**1**), epiclusianone (**2**), garciniaphenone (**3**), 2,2′,4-trihydroxybenzophenone (**4**) and diphenylmethanone (**5**).

rationalized using single crystal X-ray diffraction (XRD) analysis [22,26,31,32]. More details concerning extract preparation, chromatographic conditions (solvent set used as eluent, stationary phase, supports) and fractioning (volume and numbers of collected fractions, joining of fractions according to similarity in TLC, subdivisions of fraction groups, wash steps), instrumentation general methods and data for UV, IR, MS, NMR and XRD analyses, including structural solving and refinement starting from XRD intensity measurements, can be found in three related papers [26,27,32]. As described before by us [25], compound **4** was synthesized by reacting salicylic acid and resorcinol and purified upon standing for seven days in the form of yellow needles, from which a suitably sized clear single crystal was selected for the XRD experiment [31]. The software ORTEP-3 [33] was used in the presentation of the crystal structures of the four studied benzophenones. Diphenylmethanone (benzophenone, **5**) from Merck (Darmstadt, Germany) was also used in all the investigations.

In order to appraise the purity of benzophenone derivatives, some crystals of **1**–**4** were weighted (9–12 mg) and dissolved in methanol (10 mL), performing concentrated solutions that were used to give the following dilutions in methanol:acetic acid 5% pH 3.84 [40:60 v/v, initial mobile phase for High Performance Liquid Chromatography (HPLC) running]: 40.0, 10.0 and 0.5 mg L^{-1}. From each previous dilution, a volume of 20 μL (loop capacity) was injected in triplicate in the HPLC device (Shimadzu Corporation, Kyoto, Japan) equipped with two pumps (LC-10ATvp) and diode array detector (SPD-M10Avp) set at 254 nm. The analytical column was a C18 (150 mm × 4.6 mm) with 5 μm particle size protected by a compatible guard column. The suitable gradient was achieved using methanol:acetic acid 5% pH 3.84 (40:60 v/v) to methanol 100% in 10 min with a solvent flow rate of 1.2 mL/min at 30 °C. Prior to pumping of the mobile phase to column, the acetic acid solution and methanol were filtered under vacuum using Millipore filter and degassed separately through He sparging directly in each storage recipient. ClassVP-LC10 software was used for data collection and acquisition. The HPLC analyses of each benzophenone at the three dilutions above described have presented chromatograms with just a single strong peak. The means ± standard deviation of the percent areas in all dilutions were 98.3 ± 1.5, 99.8 ± 0.2, 98.6 ± 1.1 and 96.9 ± 0.9%, respectively for **1**–**4**.

3. Pharmacology

Benzophenone-type compounds **1**–**5** were tested for their potential to inhibit papain, trypsin, CatB and CatG by spectrofluorometric measurements. Enzymatic inhibition data were stated as compound concentrations to decrease 50% enzymatic activity (IC_{50} values), which have been calculated by time-course dose–response curves using five inhibitor concentrations. From the same time-course experiments, the pseudo first-order rate constants for enzyme inhibition, K_{obs}, were obtained. Assays to verify the inhibition reversibility were performed in the presence of increasing substrate concentrations and by the protocol where a dithiothreitol (DTT) treatment is applied. Leupeptin (LP), chymostatin, 1-[[(L-*trans*-epoxysuccinyl)-L-leucyl]amino]-4-guanidinobutane (E-64) and soybean trypsin inhibitor (SBTI) were used as reference inhibitors in the trials of CatB, CatG, papain and trypsin, respectively.

4. Results and discussion

As can be viewed in Table 1, a display of IC_{50} values, one of the benzophenone derivatives, compound **1**, has avidly inhibited all assayed enzymes with different degrees of selectivity for the proteases, binding preferentially to CatG. It is important to highlight that its IC_{50} value (2.7 ± 0.1 μM) against CatG is almost the same to that one obtained from the classical inhibitor of serine proteases, chymostatin (2.1 ± 0.1 μM). On CatB, papain and trypsin, this last benzophenone derivative was also the most active compound, with quantitative inhibitory effects that potentiate it as antiproteolytic drug. The IC_{50} values of compound **1** on the former enzymes were 2.1 ± 0.2, 1.9 ± 0.1 and 9.4 ± 0.3 μM, respectively. These data reveal that compound **1** is less active than the classical inhibitors investigated for each one of the three peptidases, leupeptin for CatB (IC_{50} 0.047 ± 0.003 μM), E-64 for papain (IC_{50} 0.047 ± 0.004 μM) and SBTI for trypsin (IC_{50} 0.109 ± 0.007 μM). All these three enzymes are known as trypsin-like hydrolases due to S1 specificity for both Arg and Lys basic residues, cleaving the C–N bond of substrate carbobenzyloxy-Phe-Arg-(7-amino-4-methylcoumarin) (Z-FR-AMC) between the Arg amino acid and AMC group [34]. Although compound **1** has strongly polarized groups as carbonyl and hydroxyl ones, anyone of its structural motifs does not resemble guanidinium and ε-amino side chains of Arg and Lys

Table 1
Quantitative in vitro inhibitory effect of natural and synthetic benzophenone derivatives on cysteine proteases Cathepsin B (CatB) and papain and serine peptidases Cathepsin G (CatG) and trypsin

Compound	IC_{50} values[a] (μM)			
	CatB	Papain	CatG	Trypsin
Guttiferone A (**1**)	2.1 ± 0.2	1.9 ± 0.1	2.7 ± 0.1	9.4 ± 0.3
Epiclusianone (**2**)	73.7 ± 5.8	19.5 ± 1.8	37.9 ± 2.1	20.1 ± 1.7
Garciniaphenone (**3**)	103.5 ± 4.4	130.8 ± 4.8	97.6 ± 5.2	103.5 ± 8.5
2,2′,4-Trihydroxybenzophenone (**4**)	198.0 ± 10.7	693.1 ± 63.0	433.2 ± 25.5	301.4 ± 7.7
Benzophenone (**5**)	288.8 ± 22.2	3465 ± 693	ND[b]	3466 ± 315
Leupeptin (LP)[c]	0.047 ± 0.003			
E-64		0.047 ± 0.004		
Chymostatin			2.1 ± 0.1	
SBTI				0.109 ± 0.007

[a] Each IC_{50} value represents the mean ± standard deviation of triplicate and the analytical and reacting conditions can be found in Section 6.
[b] ND: IC_{50} value not established by the sensitive method employed.
[c] The compounds LP, E-64, chymostatin and SBTI were used as reference inhibitors of the corresponding proteases where they have been assayed.

amino acids, respectively, which are required preferentially for substrate binding to enzymatic S1 site. This potential non-peptide antiproteolytic natural product evaluated in this work presents emphasized hydrophobicity, an essential structural feature that allows us to correlate the moderately high inhibitory activity of **1** on trypsin-like proteases with weak interactions occurring into S1 pocket as a result of low chemical compatibility between the inhibitor and residues owning acid side groups at this site. On the other hand, CatG, a chymotrypsin-like proteinase which keeps S1 specificity for hydrophobic amino acid residues, is selectively inhibited by compound **1** at quite low concentrations, in agreement with its nonpolar character that favors the anchoring. Further on, a discussion more detailed relating other structural motifs of benzophenone derivatives with CatG inhibition can be found.

The activities of **1** against all enzymes were approximately 2–69 folds higher than that manifested by compounds **2** and **3**, the other natural polyprenylated benzophenones that also inhibited significantly the four enzymes. On the other hand, the synthetic derivatives **4** and **5** were able to break weak the enzymatic property just at high dosages. In an inhibitory concentration range similar to that described for **1** by us, the natural biflavones 2,3-dihydroamentoflavone and hinokiflavone are reported as reversible inhibitors of CatB [35]. On this point, an interesting structure–activity relationship can be stated: the capacity to inhibit the enzymatic activity increases according to number of prenyl groups attached at the diphenylmethanone moiety. With regard to CatG inhibition, compound **1**, a pentaprenylated benzophenone, is about 14, 36 and 160 folds more active than the tetraprenylated (**2**), triprenylated (**3**) and nonprenylated (**4**) compounds, respectively. In agreement with these results, the CatG-inhibitory ability of **1** is very greater than that of the nonprenylated compound **5**. The ratio between quantitative inhibitions of **1** and **5** was not possible to estimate in view of the IC_{50} value of **5** to have not been established by the sensitive method employed. The approximated inhibition ratios between **1** and **2**; **1** and **3**; **1** and **4**; **1** and **5** were respectively 35:1, 49:1, 94:1 and 138:1 for CatB; 10:1, 69:1, 364:1 and 1824:1 for papain; 2:1, 11:1, 32:1 and 368:1 for trypsin, strengthening the relationship between the prenyl group number bonded to benzophenones and their antiproteolytic properties.

Nevertheless, the natural compounds **2** and **3** have presented quite more potent antiproteolytic activity than the synthetic ones **4** and **5** (about 2–178 times). These biological differences can be explained when we compare the crystalline structures of compounds **1**–**3** with **4**, once electronic and conformational features are described for all tested natural benzophenones, which are not seen in **4**. These polyprenylated compounds have a planar chelating six-membered cyclic system electronically delocalized, formed by two oxygens, where one of them is bonded to carbon bridging the substituted phenyl and bicyclic rings and another oxygen is linked to second carbon from bicycle[3.3.1]nonane moiety, a hydroxyl hydrogen atom participating in intramolecular noncovalent and covalent bonds and three carbons connecting the two oxygen atoms, where one of them is the bridge carbon and the other two are from bicycle rings, C2 and C3. The referred chelating cycle is almost entirely planar in compounds **1**–**3** in view of the highest calculated deviations from the least-squares plane passing through the six cyclic atoms aforementioned to be −0.046(3), −0.058(5) and −0.043(3) Å for bridge carbons of **1**–**3**, respectively. However, in compound **4**, the carbonylic C-atom has been deviated −0.135(1) Å from the better fitted least-squares plane passing through the six atoms cyclized by an intramolecular noncovalent hydrogen bond where the *ortho*-hydroxyl group from 2,4-dihydroxyphenyl moiety is the H-donor and the carbonylic oxygen is the H-acceptor, a value that is larger than we might expect for a significantly planar system. In Fig. 2, an ORTEP-3 representation [33] of compounds **1**–**4**, the almost planar six-membered cyclic moiety, which is stabilized by an intramolecular noncovalent H-bond, can be clearly observed in structures **1**–**3**.

The two phenolic hydroxyl groups of compound **1** can also play a key role in the molecular binding of **1** to enzymatic receptor site, enhancing the affinity between the respective inhibitor and macromolecules by means of two possible interacting mechanisms: a direct one, where the aromatic OH moieties would donate and/or accept hydrogens from certain amino acid residues, likewise other dipolar, electrostatic or chelating contacts could be involved; and another indirect one, where the keto–enol tautomer of **1**, that differs from those in solid and solution states of compounds **2** and **3** and is classically rationalized with basis on electronic resonance effect offered by one of the benzene OH groups [26], would attach to proteases more strongly than otherwise a distinct tautomeric form had prevailed over one which is found. The previously mentioned keto–enol tautomeric forms of the natural benzophenones here studied were proposed by NMR spectroscopic techniques in solution state and accurately identified by XRD analyses. The crystallographically elucidated tautomers of compounds **1**–**3** are also shown in Fig. 2. Concerning the influence of an aromatic hydroxyl group on the keto–enol tautomerism of **1**, it was verified by us that the OH group located in *para*-position from aromatic ring in relation to aromatic carbon atom attaching to the carbonyl group raises a further delocalized resonance structure passing through OH_{para}–Ph–C═O. Such electronic conjugation increases the nucleophilic character of the out-of-ring plane oxygen atom, which thereby bonds covalently to a hydrogen changeably placed in the structure that could be firmly linked to other two oxygens. To make clear, such hydrogen atom is labeled H_x in Fig. 2, and the three oxygens in which this variably positioned hydrogen could be covalently linked are bonded to C2, C4 and C10 carbons. As a result, the oxygen in query, which is bonded to carbon bridging the 13,14-

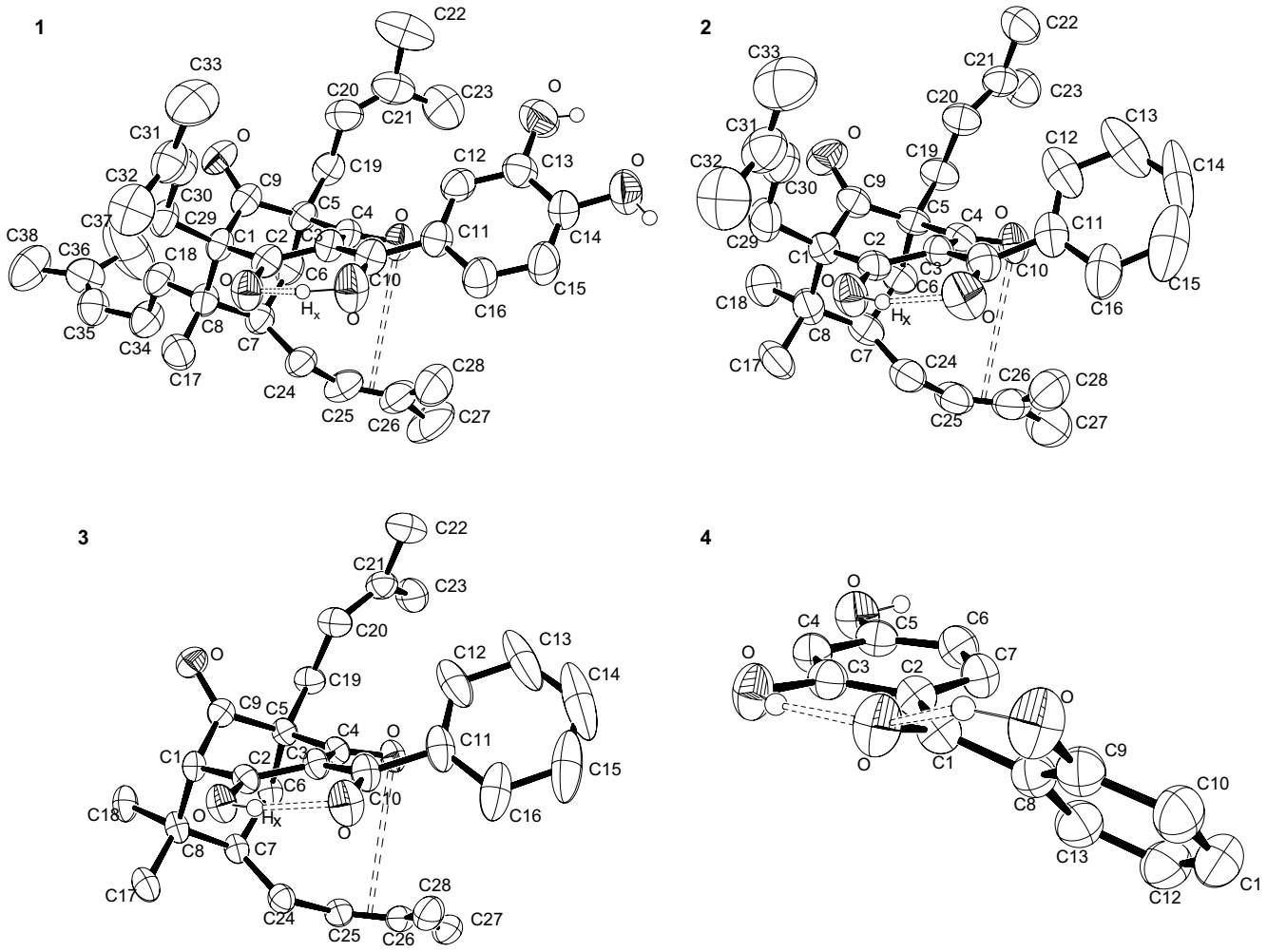

Fig. 2. An ORTEP [33] view of crystallographically determined structures of three natural polyprenylated benzophenones guttiferone A (**1**) [26], epiclusianone (**2**) [22] and garciniaphenone (**3**) [32] together with the synthetically yielded benzophenone-type derivative 2,2′,4-trihydroxybenzophenone (**4**) [25] where an arbitrary atom labeling is displayed. Ellipsoids represent 50% probability level. Double dotted line represents either the intramolecular noncovalent hydrogen bond or the dipolar interaction between the unsaturation of the prenyl moiety attached at C7 atom and the carbonylic oxygen bonded to fourth carbon atom of the bicycle ring. The C–H H-atoms were omitted for clarity and the hydrogen atom that can be changeably placed in the structures **1**–**3** is labeled as H_x and it was accurately located in each natural benzophenone using residual density maps obtained by difference Fourier synthesis during the single crystal XRD analyses [25,26,32].

dihydroxylated phenyl and bicyclo[3.3.1]nonane-2,4,9-trione moieties, is featured as hydroxylic one instead of carbonylic oxygen that is noted in **2** and **3**. Indeed, the tautomeric form of **1** is different from those of compounds **2** and **3** and this dynamic feature can be crucial for detached inhibitory activity of **1** on serine and papain proteases, as it can be observed in Fig. 3, a molecular representation of compound **1** computationally docked on the active site of CatG. The hydrogen bond involving Lys217 and the hydroxyl group at C10 as hydrogen acceptor and donor [O–H10(**1**)···$O_{backbone}$(Lys217) distance is 1.856 Å], respectively, agrees with the former hypothesis concerning the influence of keto–enol tautomeric form of compound **1** to its highest antiproteolytic activity, once the hydroxyl group at C10 is sterically able to donate the hydrogen atom to backbone carbonyl group of Lys217. On the other hand, in compounds **2** and **3**, where a carbonyl moiety takes place at this position and the hydrogen atom of keto–enol six-membered cycle is covalently bonded to oxygen atom at C2, the H-bond in query between the inhibitors and CatG was not pointed out by flexible docking simulations. Specific tautomers of protease inhibitors are required for favorable interaction between anchoring groups and the amino acids of active site, such as Asp189, a critical residue for substrate/inhibitor binding to trypsin-like serine proteases [36]. Furthermore, the additional resonance effect occurring only in **1** influences several bond angles and lengths and torsional deviations in whole molecule, as the torsional angle between the bridge hydroxyl group and the least-square plane through aromatic ring. For **1**, a torsional angle of 31.1(5)° is observed, whereas for **2** and **3** these corresponding values are 37.3(7)° and 43.7(3)°, respectively. This decreased twisting for **1** can be viewed as a consequence of electronic conjugation offered by 13,14-dihydroxyphenyl group in resonance with bridge hydroxyl group, which aligns the query groups. With regard to this point, another important SAR statement can be postulated: the inhibitory activity of natural benzophenones on the assayed proteases increases proportionally according to planarity enhancement between bridge hydroxyl/carbonyl and 13,14-dihydroxyphenyl/phenyl groups. After flexible docking, the torsional angle between the bridge group and the least-square plane through aromatic ring of compounds **1** and **3**, 25.9° and 39.9°, respectively, is lower than the respective values reported by XRD analysis, which strengthens our statement regarding the relationship between planarity and inhibitory effect. On the other hand, for compound **2**, the dihedral angle in query is 40.3°, a value slightly more opened than that one measured at solid state, which is 37.3(7)°. A suitable orientation between hydrophobic motifs from enzymes and inhibitors can be the reason of the above commented planarity to be required for high inhibitory activity. Whereas the

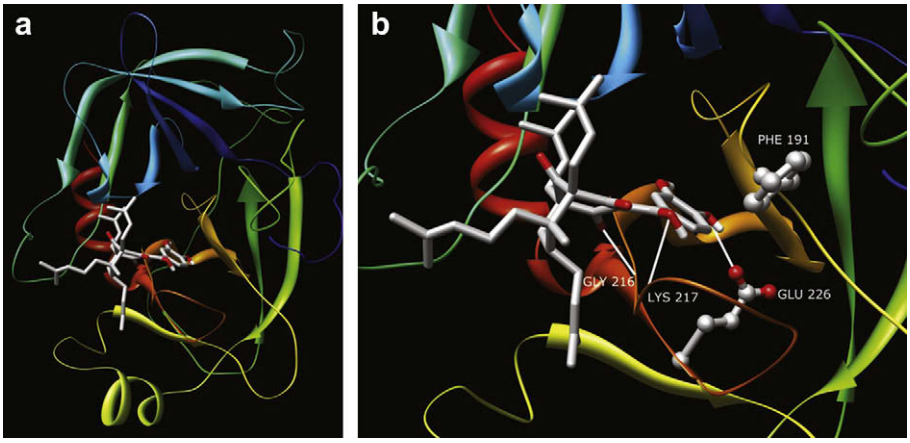

Fig. 3. Best docking orientation for compound **1** inside the active site of Cathepsin G. a. A full view of complex inhibitor–CatG. b. The hydrogen bonds that contribute for inhibitor anchoring are shown as white lines. Phe191 and Glu226 side chains were highlighted due to their key roles in the binding of inhibitor. Gly216 and Lys217 side chains are not displayed in the illustration, once the H-bonded groups of these amino acids are in the peptide chain backbone (α-amino and carbonyl groups from Gly216 and Lys217, respectively). The C–H H-atoms were omitted for clarity.

keto–enol six-membered cyclic core would anchor the inhibitor in enzyme active site by electrostatic, hydrogen and covalent (see infra) bonds, the phenyl moiety, at adequate orientation, would stack with nonpolar groups of certain amino acid residues by van der Waals, hydrophobic and π–π contacts. This hypothesis is strengthened taking into account the selective binding of compound **1** to CatG, a chymotrypsin-like protease that preferentially cleaves the peptide bond of fluorescent substrate (*ortho*-aminobenzoic acid)-AIAFFSRQ-[*N*-(ethylenediamine)-2,4-dinitrophenyl amide] (Abz-AIAFFSRQ-EDDnp) between two Phe residues after their benzyl side chains to be specifically recognized by S1 site in the enzyme [34,37]. At this subsite, there are two key residues, Phe191 and Glu226, pocketing the hydrophobic and polarized groups of substrate/inhibitor, respectively. The docking simulations have modeled a partial interaction of certain peptide substrate benzyl groups which do not fit completely in S1 pocket due to their unfavorable conformational features hindering sterically the phenyl stacking [37]. Putatively, the high coplanarity between the 13,14-dihydroxyphenyl and hydroxymethylene groups as a consequence of further electronic resonance in compound **1** allows the entire entry of dihydroxy-substituted phenyl group into S1 subsite of CatG by means of thermodynamically optimized and aligned contacts between Phe191 and the inhibitor benzene moiety, as well as the 14-hydroxy aromatic substituent could contribute to overall anchoring through electrostatic bindings and hydrogen donations to Glu226, basing the greatest in vitro anti-proteolytic effect of compound **1** on CatG. These previous statements are supported by flexible docking analyses (Table 2 and Fig. 3), which have shown two tight van der Waals (VDW) contacts between Phe191 and substituted phenyl ring of compound **1** [The C15(**1**)···H2′$_{ar}$(Phe191) and C16(**1**)···H3′$_{ar}$(Phe191) distances are equal to 2.28 and 2.51 Å, respectively], a hydrogen bond between Glu226 and 14-hydroxy substituent at *para*-position from phenyl ring in relation to aromatic carbon atom attaching the bridge group [O–H14(**1**)···O3′(Glu226) interaction length is 2.392 Å], and another H-bond between Gly216 and carbonyl oxygen atom at C4 [N–H$_{backbone}$(Gly216)···O4(**1**) distance measures 1.924 Å]. The contribution of the prenyl groups for compound **1** binding to CatG was also proved by docking simulations: there are various VDW contacts between CatG and the three prenyl groups including the atoms C19–C23 (four contacts, two of them performed by an unique hydrogen atom at C22 and the others were established by C22 atom), C24–C28 (twelve contacts, one of the hydrogen atoms at C28 has performed two contacts, another of them has contributed with three interactions and the carbon atom in which these two hydrogens are bonded has also participated with three VDW bonds; one hydrogen atom at C24, C24, C25 and C26 interacted one time each) and C29–C33 (five contacts, two of them performed by an unique hydrogen atom at C33 and another bond was established by a different hydrogen atom at C33; the last two interactions were done by C33 carbon atom). In addition, the theoretical binding results were highly correlated with in vitro inhibitory assays. The docking parameters are also displayed in Table 2, together with details of van der Waals and hydrogen bonds. Compound **1** showed a higher docking score, very likely due to the two hydroxyl groups interacting with CatG active site as well as additional hydrophobic contacts. Furthermore, guttiferone A (**1**) resembles the classical inhibitor of CatG, chymostatin, strengthening the idea of its selective binding to the active site residues.

To check the kinetic profile of the hydrolysis inhibition by three natural benzophenone derivatives which have presented promising IC_{50} values claiming further experiments, the conversion of Z-FR-AMC into AMC was monitored during 30 min. As can be appraised in Fig. 4, papain and trypsin were quickly inhibited by compounds **1**–**3**. The proteolytic activities have already attained the minimum values within approximately 5 min of incubation using the three natural benzophenones, keeping practically constant residual enzymatic activity for whole period of kinetic assay. This inhibition in a short interval time can be related with the restricted confirmations that are permitted for the structures **1**–**3**, favoring an inhibitor directing towards binding site faster than otherwise the benzophenones might bend freely. Therefore, the interactions between the verified inhibitors and trypsin-like proteases are easily stabilized and consequently the inhibition process does not delay, as it was reported by means of this time-dependent inhibition assay. In fact, it is important to emphasize that all conformational data may be correlated to the enzymatic inhibition results taking into account the marked presence of highly conjugated and electronically delocalized systems and noncovalent intramolecular hydrogen bonds in the benzophenone derivatives, along with a intramolecular dipolar interaction between the unsaturation of the prenyl moiety attached at C7 atom and the carbonylic oxygen bonded to fourth carbon atom of the bicycle ring which contributes to conformational stabilization (Fig. 2). Such structural features have been pointed out by XRD analyses and are responsible by relatively rigid conformation of assayed compounds, then allowing us to state structure–activity relationships based on torsional deviations between certain groups and presumed flexibility, as it can be found throughout the text.

Table 2
Distances of van der Waals contacts and hydrogen bonds in the CatG–compound **1** complex and the docking parameter of three natural polyprenylated benzophenones on CatG

*CatG–compound **1** van der Waals contacts*[a]		
Atom of compound **1**	Amino acid residue of CatG	Distance (Å)
H10	Lys217	2.591
H17a	Ser218	1.339
H17a	Ser218	2.420
H33b	Lys192	1.849
H33c	Lys192	1.116
H33c	Lys192	2.105
H24a	Gly216	1.801
H28a	Phe172	1.700
H28a	Phe172	2.529
H28b	Gly216	2.147
H28b	Gly216	2.413
H28b	Phe172	1.675
H22b	Hip57	2.196
H22b	Hip57	2.583
C16	Phe191	2.512
C15	Phe191	2.280
C13	Tyr215	2.556
C17	Ser218	2.073
C17	Ser218	3.151
C33	Lys192	1.771
C33	Lys192	2.804
C24	Gly216	2.535
C25	Lys217	2.439
C26	Lys217	2.282
C28	Phe172	1.928
C28	Phe172	2.946
C28	Gly216	2.906
C22	Hip57	2.988
C22	Hip57	3.035
O2	Ser218	1.955
O2	Ser218	2.614
O2	Ser218	2.281
O2	Ser218	2.672
O10	Ser218	1.911
O10	Ser218	2.931
O4	Tyr215	1.807
O4	Tyr215	2.806
*CatG–compound **1** hydrogen bonds*		
Hydrogen donor	Hydrogen acceptor	Distance (Å)
N–$H_{backbone}$(Gly216)	O4(**1**)	1.924
O–H10(**1**)	$O_{backbone}$(Lys217)	1.856
O–H14(**1**)	O3′(Glu226)	2.392
CatG–inhibitor docking score[b]		
Compound **1**	Compound **2**	Compound **3**
66.5	61.5	65.2

[a] The letters a, b and c label different hydrogen atoms bonded to a same carbon.
[b] Higher docking scores correlate more favorable binding between inhibitor and enzyme.

The adding of increasing Z-FR-AMC concentrations to reacting mixture has not recovered the activities of trypsin and papain, enzymes which are considered as models for serine and cysteine proteases' inhibition investigations, respectively, in the presence of compounds **1** and **2**, SBTI, a irreversible serine protease inhibitor under the employed analytical conditions, and E-64, a covalently bonded cysteine protease inhibitor, highlighting that the last two classical inhibitors were used as irreversible controls for each corresponding proteinase, SBTI on trypsin and E-64 on papain (Fig. 5). Differently of previous findings, the inhibitory effect of compounds **3**–**5** is disappeared competitively by addition of increasing substrate concentrations. These data led us to conclude that compounds **1** and **2** are noncompetitive inhibitors of serine and cysteine proteases, whereas compounds **3**–**5** are reversible competitive ones, accounting the much lowered inhibitory property of synthetic benzophenones **4** and **5** on both proteinase classes. The reason for reversible inhibition mode of natural compound **3** can be in its substitution pattern and conformational

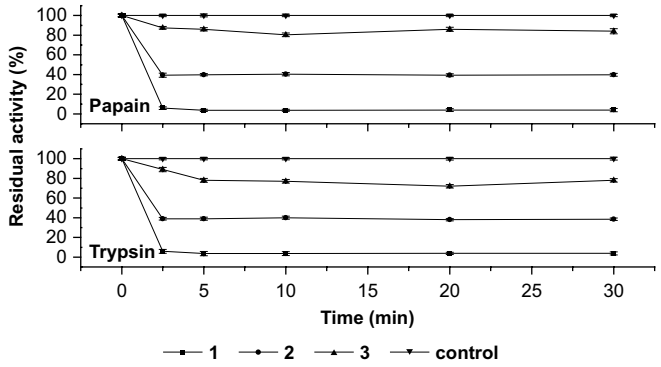

Fig. 4. Kinetic profile at 25 °C of papain and trypsin inhibitions by natural polyprenylated benzophenones. The final enzyme and inhibitor concentrations and added Z-FR-AMC solutions were respectively 3.5 nM, 9 μM and 3.1 μM for papain (buffer: sodium phosphate 50 mM pH 6.8 and EDTA 1.0 mM), and 19 nM, 10 μM and 10 μM for trypsin (buffer: Tris–HCl 50 mM pH 7.5 and $CaCl_2$ 10 mM). Each value represents the mean ± s.e.m. of three independent assays.

features: a hydrogen atom attached at the first carbon atom from bicycle moiety instead of a prenyl group like in compounds **1** and **2**, and the non-coplanarity between bridge carbonyl and phenyl groups. These structural characteristics weaken the overall interactions between compound **3** and binding site of the enzymes in comparison with the respective contacts performed by compounds **1** and **2**, culminating in the inhibitor displacement by the substrate at increasing dosages.

Results in keeping with the previous competitive inhibition experiment were obtained by treatment of papain–inhibitor complex with DTT, a reducing agent which can reactivate the oxidized cysteine proteases by leading catalytic Cys residue to thiol form. In this trial, the substrate hydrolysis was not restored after DTT adding where compounds **1**, **2** and E-64 were incubated (Fig. 6). In an opposed behavior, the papain was reactivated by reducing thiol DTT in the presence of benzophenones **3**–**5**, and the

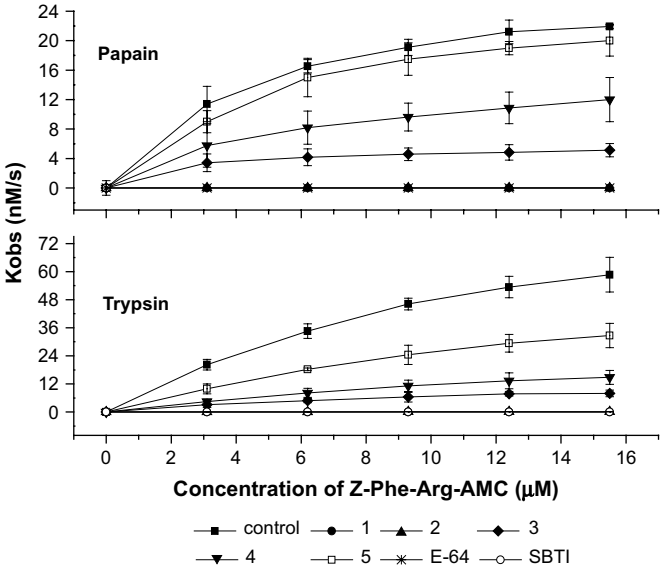

Fig. 5. Reversibility assay for papain and trypsin inhibitions by benzophenone derivatives with increasing substrate concentrations. Assayed concentrations: inhibiting benzophenones (50 μM), substrate Z-FR-AMC (3.1–15.5 μM, addition after 5 min of incubation at 25 °C), E-64 (0.2 μM) for papain (8.0 nM, buffer: sodium phosphate 50 mM pH 6.8 and EDTA 1.0 mM), SBTI (0.72 μM) for trypsin (56 nM, buffer: Tris–HCl 50 mM pH 7.5 and $CaCl_2$ 10 mM). Each value represents the mean ± s.e.m. of three independent assays.

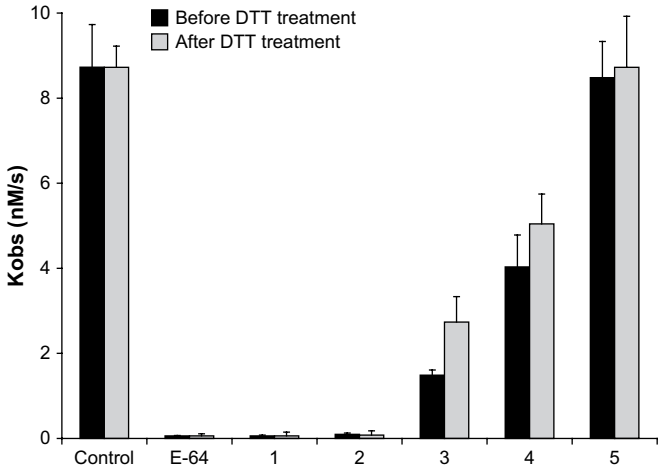

Fig. 6. Reversibility assay for papain inhibition by benzophenone derivatives after dithiothreitol (DTT) treatment. Evaluated concentrations: inhibiting benzophenones (50 μM), substrate Z-FR-AMC (3.1 μM), E-64 (0.5 μM), newly activated papain (8.0 nM, buffer: sodium phosphate 50 mM pH 6.8 and EDTA 1.0 mM). A DTT solution (10 mM) was added to a reaction mixture already containing the inhibitor and the fluorescence value was measured at the moment when the substrate was added. Control: without inhibitor. The clustered columns, which represent the mean of three independent assays, lead the upper error bars (s.e.m.).

substrate cleavage degree without any inhibitor (control) was equal to that containing compound **5** after DTT reduction. So, the inhibition of cysteine proteases by compounds **1** and **2** is irreversible, in the same way that E-64 inhibits it, and the involved mechanism is not based on oxidizing events, once DTT was not able to recover the papain hydrolytic property where these three compounds were present. Meanwhile, the reactivation of the enzymatic properly is readily gotten by reducing procedure where the reversible inhibitors **3**–**5** were present.

It is known that E-64, an epoxysuccinate derivative, bonds covalently to cysteine proteases by *S*-alkylation of the cysteine residue in the active site [38]. In the case of papain, the thiolate anion from Cys25 attacks nucleophilically the carbon atoms of the epoxide ring, which are electronically deficient, resulting in the opening of three-membered cyclic ether from inhibitor and forming a covalent thioether bond between the active site and inhibitor [38]. Other noncovalent contacts contribute for anchoring of E-64 in active site of papain. Our thought is that a similar irreversible mechanism is involved in cysteine proteases' inhibition by benzophenones **1** and **2**, detaching that all above discussed noncovalent interactions (H-bonds and van der Waals contacts) are equally important for receptor–ligand complex stabilization. The sole change is in the nucleophilic attack of cysteine residue to the carbonyl carbon atoms of compounds **1** and **2** instead of epoxidic one from E-64. As a result, a thiohemiketal bond can be found in the covalently bonded complex benzophenone **1**/**2** – papain/CatB. This attack would take place at either in the second carbon atom from the bicycle moiety (compound **1**) or in the bridge carbonyl C-atom (compound **2**). We believe that these two carbonyl carbons are more susceptible to nucleophilic attack due to their highest electrophilic characters which have been verified by XRD analysis. The C═O bond lengths of corresponding carbonyl groups (1.281(4) Å for C2═O and 1.268(6) Å for C10═O in **1** and **2**, respectively) are markedly longer than the average expected value (approximately 1.22 Å), which indicates that there is an increased electronic density polarization on carbonyl double bond resulting in a pseudo-hydroxyl character of the carbonyl groups in query. Consequently, the polarization raises partial negative and positive charges around the oxygen and carbon atoms of the formed electronic dipole, respectively, potentiating the attack by nucleophiles at the partially charged carbons. As can be seen above, the carbonyl C2═O distance in **1** is larger than the C10═O length in **2**, stating the greatest electronic polarization in ketone group of **1**, which enhances the potential of nucleophilic attack on its carbon atom when compared to compound **2**. This evidence is also useful to rationalize the lowest IC_{50} values of **1** on all tested serine and cysteine proteases. Furthermore, the hypothetical reaction modeled for cysteine proteases could be also applied for CatG and trypsin inhibitions by compounds **1** and **2**, with the formation of a hemiketal derivative, once a manner of irreversible serine proteases' inhibition requires the same nucleophilic attack mechanism [38]. Several irreversible inhibitors which are nucleophilically attacked at carbonyl groups can be found in the literature, as for instance the peptide aldehyde [39], chloromethyl ketone [40] and α,β-epoxyketone [41] derivatives.

5. Conclusion

Three natural polyprenylated benzophenone derivatives have shown potential inhibitory effect on cysteine proteases CatB and papain and serine peptidases CatG and trypsin. The concentration of pentaprenylated benzophenone guttiferone A to inhibit selectively CatG is similar to that of the peptide-based classical inhibitor of this enzyme, chymostatin, which potentiates such natural product as antiproteolytic drug for treatment of diseases in which this protease is involved, as several kinds of tumors. Its usefulness for antineoplastic therapy is further emphasized when we have accounted the beneficial effect of compounds possessing the bicycle[3.3.1]-nonanetrione moiety on tumoral and cancerous cell division. Therefore, the single natural compound adds non-peptide feature that is desired for antiproteolytic drugs with the property to act by some independent and different molecular mechanisms: altering of signal transduction pathways that results in mitosis level decreasing, inhibition of enzymes involved in DNA replication and chromosome stability, and blockage of tumor growth and dissemination by CatG and CatB activity inhibition, as it was found here. In addition, the anti-HIV ability initially reported in 1992 for compound **1** and that has been later described for compound **2** in 2005 may be based on the inhibitory activity against enzymes of protease class, once the hydrolases play an essential role in HIV maturation. Meanwhile, the synthetic benzophenones **4** and **5** have not presented significant inhibitory capacity against anyone of the assayed enzymes. The natural compounds **1**–**3** bond quickly to cysteine and serine proteases, whereas the enzymatic inhibitions of **1** and **2** are noncompetitive, compound **3** inhibits competitively papain and trypsin, once its inhibitory activity is reverted by adding substrate at increasing concentrations. Moreover, using the DTT reactivation treating we proved that compounds **1** and **2** are irreversibly attached on papain through a putative covalent thiohemiketal bond formed by nucleophilic attack of Cys thiolate anion at a specific carbonyl carbon which is more susceptible to electronic acceptance in view of its highest positive partial charge among all carbonyl C-atoms of the inhibitors. Important SAR notes were stated and will be useful for molecular modeling and searching of novel potent benzophenone-type serine and cysteine protease inhibitors: the presence of the bicycle[3.3.1]-nonanetrione and 13,14-dihydroxy-substituted phenyl groups and keto–enol tautomeric form where the bridge carbon is hydroxylated enhances the enzymatic inhibitory activity, likewise this biological effect on serine and cysteine proteases improves according to number of prenyl groups attached at the diphenylmethanone moiety and the coplanarity between bridge hydroxyl/carbonyl and 13,14-dihydroxyphenyl/phenyl groups.

6. Experimental protocols

6.1. Chemicals

All enzymes were from Merck (Darmstadt, Germany), serine protease inhibitors SBTI and chymostatin along with cysteine ones E-64 and LP were commercially obtained from Sigma (St. Louis, USA). The fluorogenic substrates Z-FR-AMC and Abz-AFAFFSRQ-EDDnp were generously given by Dr. Luiz Juliano (Department of Biophysics, Federal University of São Paulo, Brazil). Substrate hydrolyses were monitored in a spectrofluorometer Shimadzu RF-1501 (Shimadzu Corporation, Kyoto, Japan) and the enzymatic molar concentrations were estimated by titration according to kinetic parameters [34].

6.2. Inhibition assays

CatB inhibition experiment was performed as previously described [34], using the fluorogenic substrate Z-FR-AMC, whose hydrolysis was spectrofluorometrically measured at 460 nm after the free AMC have been excited at 380 nm. AMC solutions were used as working standards to generate a calibration curve and the substrate has been prepared diluting several times a stock solution at 1 mg/mL of water:dimethylformamide (50:50 v/v) in the CatB buffer composed of Tris–HCl 50 mM (pH 7.5) and ethylenediaminetetraacetic acid (EDTA) 5 mM. For the tested inhibitors, each benzophenone was dissolved in dimethyl sulfoxide (DMSO) and diluted with enzymatic buffer (0.5–280 μM). These solutions were added to the buffer containing the respective enzyme previously treated with DTT 10 mM, and the resulting mixture was incubated for 5 min at isothermal 25 °C on spectrofluorometer. The enzymatic reaction was started by adding of fluorescent substrate solution at 5.2 μM to the cuvette. The final concentration of CatB in the reactant mixture was 1.0 nM and LP was used as classical inhibitor of this protease. The same laboratorial protocol was adopted for the assays with papain, trypsin and CatG, with some different experimental parameters as follows. Papain: buffer composed of sodium phosphate 50 mM (pH 6.8) and EDTA 1.0 mM, Z-FR-AMC fluorescent substrate solution was 3.1 μM, final enzymatic concentration was 7.8 nM, E-64 was used as classical inhibitor; Trypsin: buffer composed of Tris–HCl 50 mM (pH 7.5) and $CaCl_2$ 10 mM, Z-FR-AMC fluorescent substrate solution was 3.1 μM, final enzymatic concentration was 56.1 nM, SBTI was used as classical inhibitor; CatG [37]: Hepes buffer 50 mM (pH 7.4) containing NaCl 50 mM, the solution concentration of an internally quenched fluorogenic peptide Abz-AIAFFSRQ-EDDnp, where Abz is the fluorescent donor and EDDnp is the fluorescent quencher (emission and excitation wavelengths for Abz were λ_{em} and $\lambda_{ex} = 320$ nm), was 1.7 μM, which was spectrally computed through electromagnetic absorption of 2,4-dinitrophenyl moiety, benzophenones' concentration ranging from 0.5 to 240 μM, final enzymatic concentration was 9.9 nM, chymostatin was used as classical inhibitor. For serine proteases trypsin and CatG, the initial treatment with DTT has not been applied.

6.3. Kinetic profile of inhibitions

To obtain the kinetic profile of the enzymatic inhibitions, the same procedure was performed for papain and trypsin using the buffers of each protease and fixed concentrations of benzophenones **1**–**3**. The fluorescent emissions originating from peptide substrate hydrolyses were quantified at 0, 2 min 30 s, 5, 10, 20 and 30 min after the addition of Z-FR-AMC to newly incubated cuvette (1 mL) already containing the enzymes and inhibitors diluted in the respective buffers. For this trial, the final enzyme and inhibitor concentrations and added Z-FR-AMC solutions were respectively 3.5 nM, 9 μM and 3.1 μM for papain, and 19 nM, 10 μM and 10 μM for trypsin.

6.4. Reversibility evaluation

In order to recognize whether the benzophenone derivatives could bond either irreversibly or reversibly to the enzyme active site, papain and trypsin, models for cysteine and serine proteases, respectively, were also competitively inhibited by compounds **1**–**5** at 50 μM in the presence of increasing Z-FR-AMC concentrations (3.1–15.5 μM). E-64 (0.2 μM) and SBTI (0.72 μM) were comparatively used in the assays of papain (8.0 nM) and trypsin (56 nM), respectively. The reversibility of papain inhibition was evaluated by fluorescence measurement of a reaction mixture treated with DTT solution (10 mM) after either the benzophenones (50 mM) or E-64 (0.5 mM) were already incubated. Such procedure is able to reactivate the enzymatic catalysis if the inhibition was reversibly based. These tests were matched with the ones in which inhibitor was absent, and all trials were begun when the Z-FR-AMC solution (3.1 μM) has been added to the mixtures with or without DTT.

6.5. Computational docking

The GOLD program (version 3.1.1) [42] has been used and the default parameters were set: population size 100, selection-pressure 1.1, number of operations 100,000, number of islands 5, niche size 2, docking runs 5 and operator weights for migrate, mutate and crossover were 10, 95 and 95, respectively. The binding site of compounds **1**–**3** was defined as all the residues within 10 Å from one of the carboxylate oxygens of Glu226. The GoldScore fitness function was selected for scoring the docking poses. The coordinates for cathepsin G, where the complexed succinyl-Val-Pro-Phe^P-$(Oph)_2$ inhibitor (Oph_2 is a diphenyl ester) was first removed, from Brookhaven Protein Data Bank (PDB code 1cgh) were downloaded [43]. For compounds **1**–**3**, the geometries determined by the X-ray diffraction analysis were used as input without further optimization. Early run terminations with only three chromosomes within 1.5 Å rmsd of each other were not reached in all simulations.

Acknowledgements

We thank the Brazilian Research Council CNPq (Conselho Nacional de Desenvolvimento Científico e Tecnológico) and CAPES (Coordenação de Aperfeiçoamento de Pessoal de Nível Superior) for research fellowships (ACD and FTM), FAPEMIG (Fundação de Amparo à Pesquisa do Estado de Minas Gerais Proc.: EDT-3310/06), CAPES and FINEP (Financiadora de Estudos e Projetos – Proc.: 1110/06) for financial support.

References

[1] K. Brocklehurst, F. Willenbrock, E. Salih, in: A. Neuberger, K. Brocklehurst (Eds.), New Comprehensive Biochemistry, Elsevier, Amsterdam, 1987, pp. 39–158.
[2] T. Taniguchi, T. Mizuochi, T. Towatari, N. Katunuma, A. Kobata, J. Biochem. 97 (1985) 973–976.
[3] H. Kirschke, A. Barret, in: B. Glaumann (Ed.), Lysosomes: Their Roles in Protein Breakdown, Academic Press, London, 1987, pp. 193–238.
[4] A. Barrett, Biochem. J. 131 (1973) 809–822.
[5] J. Mort, A. Recklies, Biochem. J. 233 (1986) 57–63.
[6] L. Polgar, C. Csoma, J. Biol. Chem. 262 (1987) 14448–14453.
[7] B.E. Cathers, C. Barret, J.T. Palmer, R.M. Rydzewski, Bioorg. Chem. 30 (2002) 264–275.
[8] J.E. Koblonski, B.F. Ahram, B.F. Sloane, Clin. Chim. Acta 291 (2000) 113–135.
[9] M. Baggiolini, U. Bretz, B. Dewald, M.E. Feigenson, Agents Actions 8 (1978) 3–10.
[10] A.J. Barrett, Methods Enzymol. 80 (1981) 561–565.
[11] W. Watorek, D. Farley, G. Salvesen, J. Travis, Adv. Exp. Med. Biol. 240 (1988) 23–31.

[12] J.G. Bieth, in: R.P. Mecham (Ed.), Biology of the Extracellular Matrix, Academic Press, New York, 1986, pp. 217–320.
[13] C.A. LaRosa, M.J. Rohrer, S.E. Benoit, L.J. Rodino, M.R. Barnard, A.D. Michelson, J. Vasc. Surg. 19 (1994) 306–318.
[14] O. Chertov, H. Ueda, L.L. Xu, K. Tani, W.J. Murphy, J.M. Wang, O.M. Howard, T.J. Sayers, J.J. Oppenheim, J. Exp. Med. 186 (1997) 739–747.
[15] T. Yamazaki, Y. Aoki, Immunology 93 (1998) 115–121.
[16] M. Padrines, M. Wolf, A. Walz, M. Baggiolini, FEBS Lett. 352 (1994) 231–235.
[17] C.M. Maison, C.L. Villiers, M.G. Colomb, J. Immunol. 147 (1991) 921–926.
[18] D.H. Allen, P.B. Tracy, J. Biol. Chem. 270 (1995) 1408–1415.
[19] S. Yui, K. Tomita, T. Kudo, S. Ando, M. Yamazaki, Cancer Sci. 96 (2005) 560–570.
[20] R.J. Beynon, J.S. Bond (Eds.), Proteolytic Enzymes: A Practical Approach, Oxford University, Liverpool, 1989.
[21] K.R. Gustafson, J.W. Blunt, H.G.M. Munro, R.W. Fuller, C.T. McKee, J.H. Cardellina, J.B. McMahon, G.M. Cragg, M.R. Boyd, Tetrahedron 48 (1992) 10093–10102.
[22] M.H. Santos, N.L. Speziali, T.J. Nagem, T.T. Oliveira, Acta Crystallogr. C54 (1998) 1990–1992.
[23] A.J. Cruz, V.S. Lemos, M.H. Santos, T.J. Nagem, S.F. Cortes, Phytomedicine 13 (2006) 442–445.
[24] A.L. Piccinelli, O.C. Rubio, M.B. Chica, N. Mahmood, B. Pagano, M. Pavone, V. Barone, L. Rastrelli, Tetrahedron 61 (2005) 8206–8211.
[25] A.C. Doriguetto, F.T. Martins, J.A. Ellena, R. Salloum, M.H. Santos, M.E.C. Moreira, J.M. Schneedorf, T.J. Nagem, Chem. Biodivers. 4 (2007) 488–499.
[26] F.T. Martins, J.W. Cruz Jr., P.B.M.C. Derogis, M.H. Santos, M.P. Veloso, J.A. Ellena, A.C. Doriguetto, J. Braz. Chem. Soc. 18 (2007) 1515–1523.
[27] P.B.M.C. Derogis, F.T. Martins, T.C. Souza, M.E.C. Moreira, J.D. Souza Filho, A.C. Doriguetto, K.R. Souza, M.P. Veloso, M.H. Santos, Magn. Reson. Chem. 46 (2008) 278–282.
[28] D.D. Carballo, S. Seeber, D. Strumberg, R.A. Hilger, Int. J. Clin. Pharmacol. Ther. 41 (2003) 622–623.
[29] L.E. Avril, M.D.M. Ferrer, M.B. Bourdet, F. Gauthier, FEBS Lett. 367 (1995) 251–256.
[30] M.A. Navia, P.R. Chaturvedi, Drug Discov. Today 1 (1996) 179–189.
[31] Supplementary crystallographic data sets (excluding structure factors) for compounds **1**–**4** are available through the Cambridge Structural Data Base, deposition codes CCDC 643597, IUCr DA1009, CCDC 667556 and CCDC 606243, respectively. Copies of this information may be obtained free of charge from The Director, CCDC, 12 Union Road, Cambridge, CB2 1EZ, UK (fax: +44 123336 033; e-mail: deposit@ccdc.cam.ac.uk or www.ccdc.ac.uk).
[32] F.T. Martins, I. Camps, A.C. Doriguetto, M.H. Santos, J. Ellena, L.C.A. Barbosa, Helv. Chim. Acta 91 (2008) 1313–1325.
[33] L.J. Farrugia, J. Appl. Crystallogr. 30 (1997) 565.
[34] R.L. Melo, L.C. Alves, E.D. Nery, L. Juliano, M.A. Juliano, Anal. Biochem. 293 (2001) 71–77.
[35] G.Z. Zeng, X.L. Pan, N.H. Tan, J. Xiong, Y.M. Zhang, Eur. J. Med. Chem. 41 (2006) 1247–1252.
[36] B.W. Clare, A. Scozzafava, C.T. Supuran, J. Enzyme Inhib. 16 (2001) 1–13.
[37] S. Réhault, M.B. Bourdet, M.A. Juliano, L. Juliano, F. Gauthier, T. Moreau, J. Biol. Chem. 274 (1999) 13810–13817.
[38] J.C. Powers, J.L. Asgian, O.D. Ekici, K.E. James, Chem. Rev. 102 (2002) 4639–4750.
[39] T. Sasaki, M. Kishi, M. Saito, T. Tanaka, N. Higuchi, E. Kominami, N. Katunuma, T. Murachi, J. Enzyme Inhib. 3 (1990) 195–201.
[40] T. Sasaki, T. Kikuchi, I. Fukui, T. Murachi, J. Biochem. 99 (1986) 173–179.
[41] Y. Koguchi, J. Kohno, S. Suzuki, M. Nishio, K. Takahashi, T. Ohnuki, S. Komatsubara, J. Antibiot. 52 (1999) 1069–1076.
[42] Gold, version 3.1.1, Cambridge Crystallographic Data Centre, Cambridge, UK.
[43] P. Hof, I. Mayr, R. Huber, E. Korzus, J. Potempa, J. Travis, J.C. Powers, W. Bode, EMBO J. 15 (1996) 5481–5491.